International Journal of
INTELLIGENT SYSTEMS AND APPLICATIONS IN ENGINEERING
ISSN:2147-6799 www.ijisae.org Original Research Paper

# In-Vitro Detection of Tooth Decay Using Reduced Graphene Oxide (rGO) based Sensor

**[1]Payal Ghutke, [2]Wani Patil**

**Submitted**: 22/12/2023 **Revised**: 28/01/2024 **Accepted**: 08/02/2024

**Abstract:** The pH in the tooth is related to the tooth cavity, which mainly arises due to the interaction of the cariogenic bacteria with the carbohydrates present in the food. Thus, in this work, to detect the tooth cavity we have fabricated the pH sensor which comprises the interdigitated electrodes (IDEs) mounted on the electrodes on the printed circuit board. Fabricated IDEs have length and width of about 100 mm with 0.05 mm of copper acting as the electrodes. Further, rGO is used as the sensing film to detect the pH. For this purpose, rGO in powder form is converted into the liquid with the help of dispersion in the ethanol followed by sonication for about 20 minutes. Then the rGO sample is drop casted on the fabricated IDEs and subsequently air dried for 24 hrs. Further, we have taken the standard pH solution ranging from 4 to 12 and measured the sensor resistance. Further, to enhance the accuracy of the detection we have implemented the principle component analysis and k-mean algorithm on the self-collected data.

***Keywords:*** *In-situ dental applications, reduced graphene oxide, sensor resistance, ph values.*

## 1. Introduction

Tooth decay, which mainly arises due to the diminished focus on oral hygiene, leads to the fatal situation for teeth and we observe the loss of the teeth[1][2]. Tooth decay germinates due to the interaction of the carbohydrates present on the tooth and cariogenic bacteria. The byproduct generated by this bacteria is organic acid, which interacts with the tooth and hampers the balanced tooth restoration mechanism [3][4]. In order to ensure major tooth loss and to enhance the quality of life there is a dearth of mechanisms for early detection and provide instant control measures. At present, the standard testing protocol followed by the dentist consists of visual inspection and for this purpose a tool named dental explorers is widely used by the dentist[5][6]. However for the visual inspection plethora of technical acumen is required otherwise the inspection may lead to erroneous results. Beside this, it is very pivotal to establish the protocol to predict the diagnosis for the tooth cavity and provide the quantitative results. Apart from the aforementioned protocols, preventive measures has to be considered while using the dental explorers otherwise it may leads to infection or fractures [7][8].Thus, for the clinical measurements there is a dearth of the diagnostic methods, which are precise and prove the quantitative information considering the non-invasive way of detecting the tooth cavity. To abate the tooth loss due to improper prediction of the tooth cavity, researchers and dentists have explored the combination of the visual inspection with other methods such as radiographic examination [9][11], pH detection [12][13] and fluorescence [11][14]. In radiographic inspection desists get the gray-scale image, which is mapped to the density loss due to mineral content. Nevertheless, some of the primary disadvantages of this method are low selectivity and sensitivity, which hinders the accuracy of the tooth decay detection. Thus, to enhance the detection accuracy, various researchers have reported fluorescence-based inspection and pH detection methods. Interestingly, out of these two aforementioned tooth cavity detection methods, pH detection is widely preferred mainly due to the direct relation of the pH with the bacterial activity within the tooth. For pH detection in the tooth cavity, researchers have reported various sensors and electrodes systems which includes the fabrication of the antimony electrodes [15][17], pH imaging [18] and ion-sensitive field effect transistors (ISFETs) [19][21]. The major drawback of the antimony electrodes resides in the generation of the toxic elements considering the organism. pH imaging tooth cavity detection offers very accurate results but the major drawback is acquisition instrument, which is very large and it can't be practically implemented to the patients. Previously reported work shows the effect of the pH data on the tooth cavity where they also used the pH imaging instruments and mapped the data with tooth caries [19]. Advancement in the micro-sensor fabrication technology, researchers have fabricated the ISFET for the pH sensing. But the major drawback in this technology is the cost associated to fabricate the ISFET

*[1]G H Raisoni University, Amravati Research Scholar, Department of Electronics & Telecommunication Engineering India.*
*payal.ghutke@raisoni.net*
*[2]G H Raisoni College of Engineering, Nagpur Assistant Professor, Department of Electronics Engineering India*
*wani.patil@raisoni.net*

and copious data is required to understand its reliability under the clinical trials. Thus with the motivation of developing the cost-effective sensor, which can detect the pH and the measured pH can be mapped to the tooth cavity. For this purpose, first we have fabricated the interdigitated electrodes (IDEs) on the printed circuit board (PCB) where reduced graphene oxide as the sensing film. Then we have converted the rGO from powder form to solution form with the help of the ultrasound sonicator. Then, the rGO solution is drop-casted on the fabricated sensor using the micropipette. Further, we have used the standard pH sample ranging from 4 to 12 and studied the sensor response. Further, In order to improve the accuracy of the pH detection, we have implemented the k-mean and PCA algorithm on the self-connected data, which illustrates the novelty of this work.

## 2. Methods and Materials

This section illustrated the preparation of the rGO solution and the design and fabrication of the IDEs on the PCB. Then measurement set-up is explained, which is required to carry out the pH measurements. Then sensor resistance is studied with the help of the multimeter and measured data is logged into the computer. Further, the PCA and k-mean methods are used on the self-collected data to enhance the accuracy of detection.

### 2.1 rGO Sample Preparation

In this work, we have used the rGO [22], which is available in the powdered form. In order to ensure the reliable operation it is important that rGO should retain on the fabricated sensor and should not peel off during the measurements. For this purpose, it is very pivotal to convert the powdered rGO into the liquid solution which is depicted in Figure. 1. First the 10 mg of rGO is taken in the petri dish and measured its weight with the help of micro weighing balance. Further, rGO powder is poured in the test tube along with 100 ml of the ethanol as illustrated in Figure. 1. To ensure the proper dispersion of the rGO in the ethanol, the test tube is placed in the ultrasound sonicator for about 20 minutes, where the temperature in the sonicator is maintained at 25 $^{0}$C. Then the test tube is removed from the sonicator and with the help of the micro-pipette, the rGO solution is drop casted on the fabricated sensor and kept it in the air dried for about 24 hours. Then the fabricated sensor with rGO as the sensing film is ready for the further measurements.

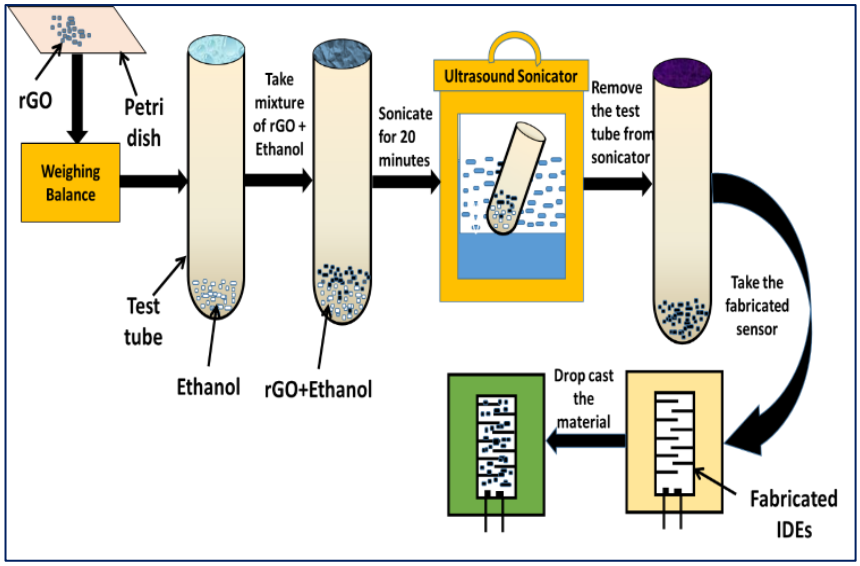


**Fig. 1** rGO solution process and drop casting on the fabricated sensor.

### 2.2 IDEs on the PCB fabrication

In order to fabricate the IDEs on the PCB we have used the standard protocols designed for printing the copper electrodes on the PCB. First the single sided copper clad bare PCB is taken and the IDE pattern are drawn in the PCB using the embossing the pattern using the hot iron pressing. Then the IDE pattern is transferred to the PCB and this pattern acts as the masking, which ensures that copper beneath the mask will retain during the etching process. Subsequently for the etching process, the PCB is inserted into the ferric chloride (FeCl2) solution and used for stirring for about 20 minutes. The stirring process in the FeCl2 removes the unexposed copper and the copper beneath the IDE mask will retain. Then the masking material is removed with the help of an isopropyl alcohol (IPA) and subsequent rinsing in the water.

### 2.3 Experimental set-up

Figure. 2 depicts the experimental set-up used in this work. Figure. 2 (a) shows the fabricated sensor which comprise the IDEs fabricated on the PCB. The length and width of the IDEs is about 1 cm and 0.5 cm,

respectively. As shown in Figure. 2 (a) the rGO is drop casted on the IDEs, which forms the pH sensor. Further, electrical contacts are taken out with the help of the silver epoxy as depicted in Figure. 2 (b). Then the sensor is connected to the multimeter, which measures the sensor change in resistance when exposed to various pH solutions ranging from 4 to 12. Micro pipette is used to drop cast the pH solution on the fabricated sensor as illustrated in Figure. 2 (b). All measurements are carried out at room temperature 25 0C and the relative humidity (RH) is maintained at 50 % RH.

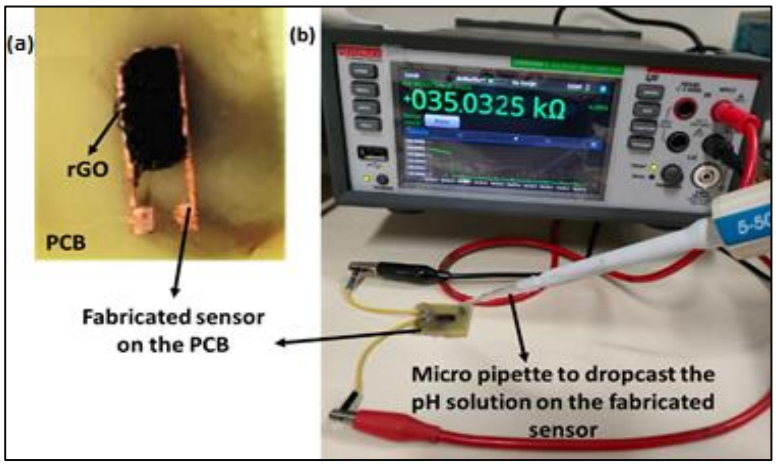


**Fig. 2** (a) rGO drop casted on the fabricated sensor, (b) Measurement set-up to record the sensor change in resistance when exposed to various pH

## 3. Results and Discussion

### 3.1 Sensor Change in Resistance for Various pH Values

In order to examine the sensor change in the resistance for various pH values ranging from 4 to 12 is explained in this section. First, we have studied the sensor change in resistance when exposed to the pH 12 sample and we have performed each measurement 4 times as depicted in Figure. 3 (a-d), respectively. As shown in Figure. 3, when the sensor is exposed to the pH solution it is referred as the "ON" and when the pH sample is removed from the solution it is termed as "OFF". From Figure. 3 (a-d) it can be inferred that the average value of the resistance of the sensor reaches the saturated value at about 26 KΩ. From Figure. 3 (a-d) it can be inferred that resistance drops when exposed to the pH solution. From Figure. 3 (a-d) it can also be concluded that a fabricated sensor offers a response time of about 10 seconds.

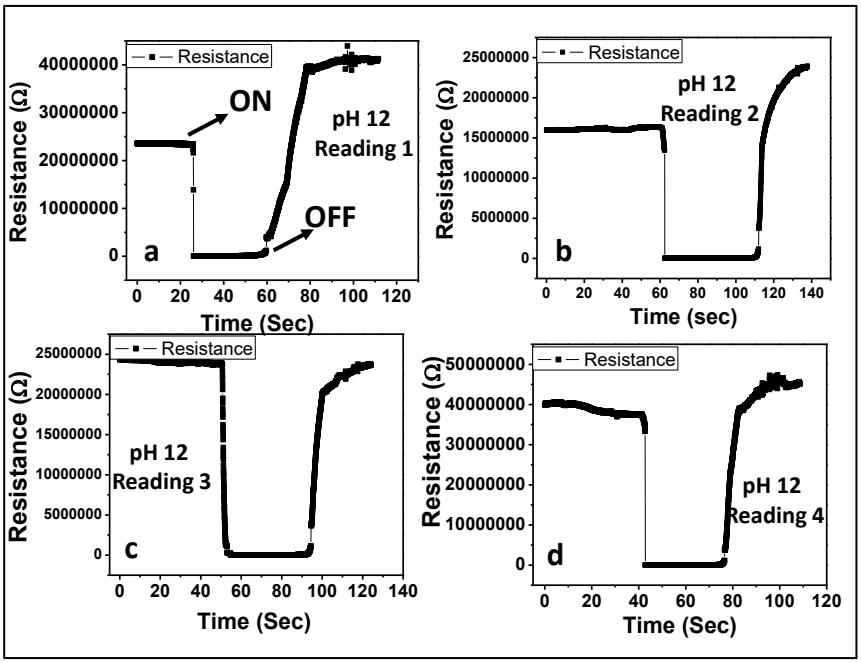


**Fig 3** Change in the sensor resistant for pH 12, which is repeated 4 times (a) reading 1, (b) reading 2, (c) reading 3 and (d) reading 4

Then, we have exposed the sensor to pH 9 and measured the sensor change in resistance which is repeated 4 times as depicted in Figure. 4 (a-d), respectively. From Figure. 4 (a-d) it can be inferred that resistance of the fabricated sensor decreases monotonically when exposed to the pH solution. Further, From Figure. 4 (a-d) it can be inferred that the average value of the resistance of the sensor reaches the saturated value at about 22.4 KΩ.

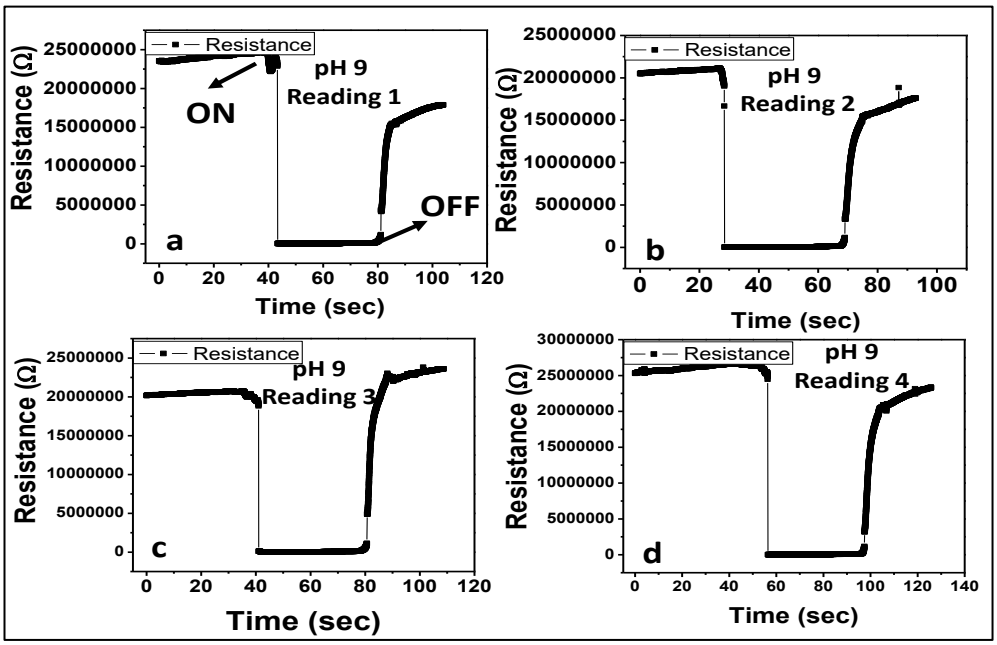


**Fig 4** Change in the sensor resistant for pH 9, which is repeated 4 times (a) reading 1, (b) reading 2, (c) reading 3 and (d) reading 4

Subsequently, the fabricated sensor is exposed to pH 7 solution and its resistance change is measured, which is repeated 4 times as depicted in Figure. 5 (a-d), respectively. Likewise we observe in the Figure. 4, in Figure. 5 (a-d) depicts the monotonic change in the sensor resistance where resistance is around 22 KΩ. From Figure. 5 (a-d) also depicts the response of the sensor, which is around 10 seconds.

Lastly, pH 4 solution is used to measure the fabricated sensor change in the resistance as depicted in Figure. 6 (a-d), respectively. pH 4 is towards the alkaline in nature observed on the pH scale. Figure. 6 (a-d) depicts the monotonic change in the sensor resistance where resistance is around 21.8 KΩ.

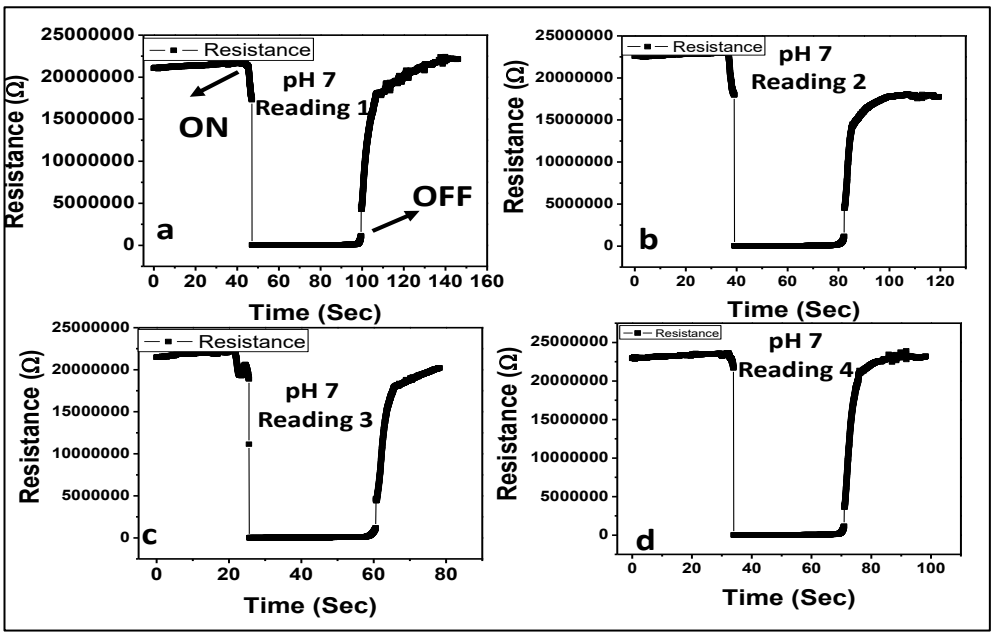


**Fig 5** Change in the sensor resistant for pH 7, which is repeated 4 times (a) reading 1, (b) reading 2, (c) reading 3 and (d) reading 4

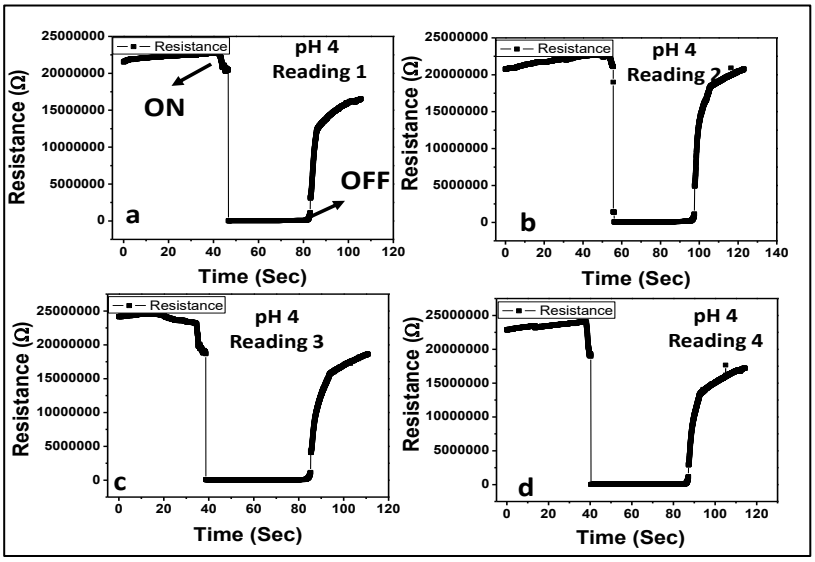


**Fig 6** Change in the sensor resistant for pH 4, which is repeated 4 times (a) reading 1, (b) reading 2, (c) reading 3 and (d) reading 4

Figure. 7 illustrates the plausible sensing mechanism, which is associated with the protonation and deprotonation of the OH groups. When the pH is low then protonation occurs which generate the positive charge (OH + H+ = OH+2), When pH is very high then negative charges are generated which leads to deprotonation (OH – H+ = O−). This leads to change in the resistivity of the sensor when pH is increased. [23]

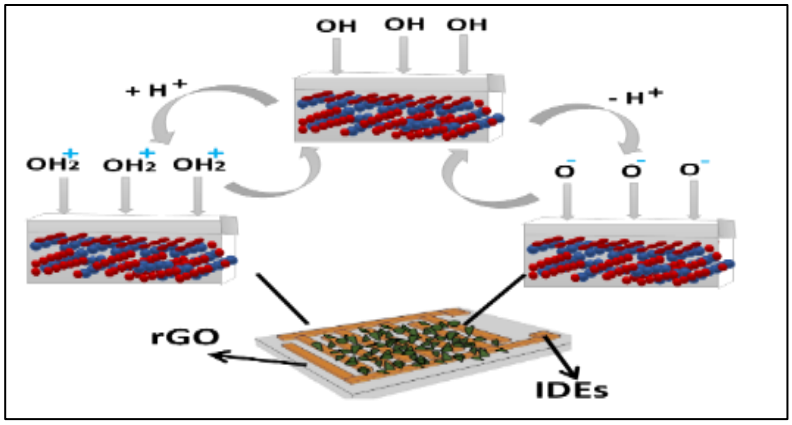


**Fig 7** Plausible sensing Mechanism

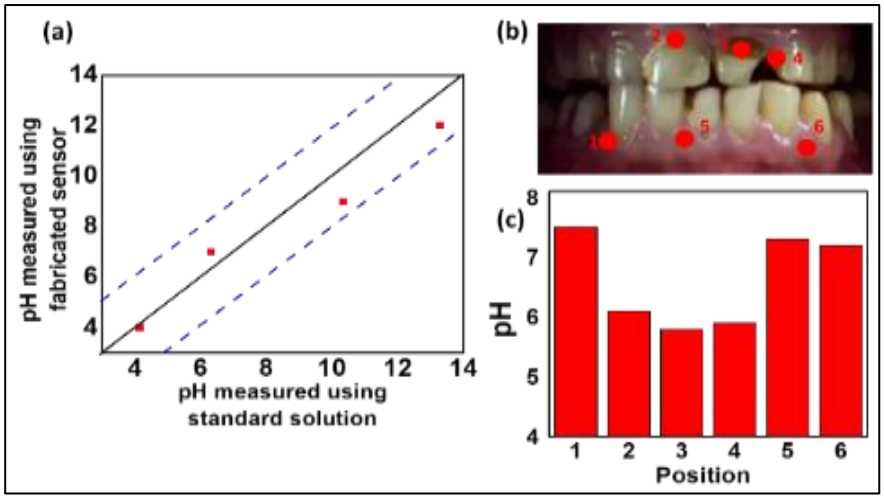


**Fig 8** (a) Benchmarking of the measured pH with standard solution,

(b) actual teeth with activity and (c) measured pH at different positions

Figure. 8 (a) depicts the benchmarking of the fabricated pH sensor with GO as the sensing film and its benchmarking with the standard pH solution. From Figure. 8 (a) it can be inferred that the absolute discrepancy between the measured pH using the fabricated sensor and standard pH solution is within ± 1 pH, which is in agreement with the reported work. Further, in order to validate the efficacy of the fabricated sensor, we have taken the pH sample from the tooth, which has decayed due to the caries as shown in Figure. 8 (b). We have randomly selected 6 positions from the tooth which has a tooth cavity and measured the pH using the fabricated sensor. From Figure. 8 (c) it is observed that, absence of the tooth cavity results in the pH vary close to 7. However, the location comprises pH, the pH drops to about 5.8. This indicates the potential use of the fabricated sensor for the tooth cavity detection.

### 3.2 PCA and k-means

PCA is an arithmetic methodology which is used for reduction of huge data sets' dimensionality without losing its information. This is possible by converting the data set to an updated set of vectors which is known as the principal components (PCs). The PCs are uncorrelated data that is ordered in such a way that the first two PCs components can be used to retain the information present in the entire original data. The experiments performed in this work are a single response pattern of 120 seconds sample points and these are converted to only two PCs. These two PCs from the experiments represent most of the information data that is present in the whole actual single response pattern. As the dimensions of the matrix are reduced further and it makes classification processes simpler in terms of data processing.

After getting PCs from PCA, the next step is the classification of the pattern to represent it as cavity or non-cavity clusters and this can be achieved by using the K-mean clustering algorithm as shown in Figure. 9. K-means is a widely used clustering algorithm where a given data set, i.e. number of time experiments is performed (N), are classified through a defined number of 'k' clusters. In our testing, 'N' is 100 and value 'k' is 4 where k is the fixed apriority that depends on the number of test samples that is required to be classified. To elaborate further to align with our experiments, 100 sets of PCs, that represent N=100 experiments, are classified into k=4 clusters as there are four various types of test samples required to be classified.

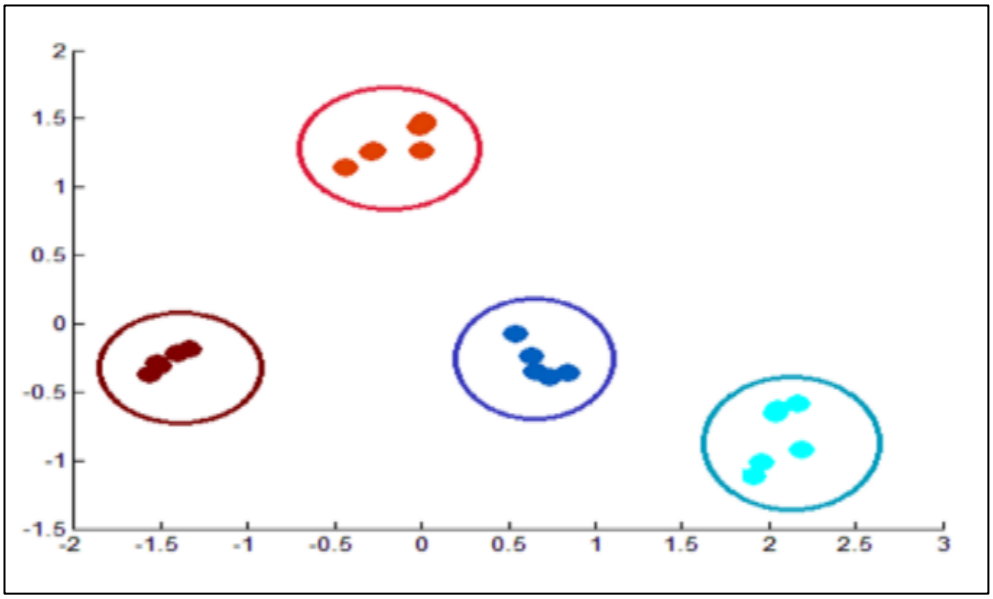


**Fig 9** PCA and K-Mean clustering showing cavity and non-cavity clusters.

## 4. Conclusion

In this work, we have examined the performance of the pH sensor where rGO is used as the sensing film. First we have fabricated the IDEs on the PCB and rGO is dropcasted on it. Then the fabricated sensor is exposed to different pH solutions ranging from 4 to 12. Further, we have observed that fabricated sensor resistance increases with increase in the pH values. Further, the lab measurement results indicate that the fabricated sensor offers the response time of about 10 seconds. Further, we explored the plausible sensing mechanism. Then we have implemented the PCA and k-mean algorithm to improve the accuracy of detection.

## References

[1] Poul Erik Petersen, Denis Bourgeois, Hiroshi Ogawa, Saskia Estupinan-Day, Charlotte Ndiaye

(2005), “The global burden of oral diseases and risks to oral health,” Bulletin of the world health organization, vol. 83, pp. 661-669.

[2] Pitts, Nigel B., “et al.” (2017), “Dental caries,” Nature reviews Disease primers, vol. 3.1 pp. 1-16.

[3] A F Paes Leme, H Koo, C M Bellato, G Bedi, J A Cury (2006), “The role of sucrose in cariogenic dental biofilm formation—new insight,” Journal of dental research, vol. 85, pp. 878-887.

[4] Selwitz, Robert H., Amid I. Ismail, and Nigel B. Pitts (2007 ),“Dental caries”, The Lancet, vol. 369, pp. 51-59.

[5] Pitts, Nigel B. (2001), “Clinical diagnosis of dental caries: a European perspective,” Journal of Dental Education vol. 65 pp. 972-978,

[6] Ismail, A. I. J. (2004), “Visual and visuo-tactile detection of dental caries,” vol. 83, pp. 56-66.

[7] Ekstrand, Kim, V. Qvist, and A. Thylstrup (1987), “Light microscope study of the effect of probing in occlusal surfaces,” Caries research, vol. 21, pp. 368-374.

[8] Juliana Mattos-Silveira, Marina Monreal Oliveira, Ronilza Matos, Cacio Moura-Netto, Fausto Medeiros Mendes, and Mariana Minatel Braga (2016), “Do the ball-ended probe cause less damage than sharp explorers?—An ultrastructural analysis,” BMC oral health, vol. 16, pp. 1-7.

[9] D N Ricketts, E A Kidd, B G Smith, R F Wilson (1995), “Clinical and radiographic diagnosis of occlusal caries: a study in vitro,” Journal of Oral Rehabilitation, vol. 22, pp. 15-20.

[10] Wenzel, A. (1998), “Digital radiography and caries diagnosis,” Dentomaxillofacial Radiology, vol. 27, pp. 3-11.

[11] Pretty, Iain A. (2006), “Caries detection and diagnosis: novel technologies,” Journal of dentistry, vol. 34, pp. 727-739.

[12] Igarashi, K., I. K. Lee, and C. F. Schachtele (1989), “Comparison of in vivo human dental plaque pH changes within artificial fissures and at interproximal sites,” Caries research, vol. 23, pp. 417-422.

[13] A Smit, M Pollard, P Cleaton-Jones, A Preston (1997), “A comparison of three electrodes for the measurement of pH in small volumes,” Caries research, vol. 31, pp. 55-59.

[14] A Lussi, S Imwinkelried, N Pitts, C Longbottom, E Reich (1999), “Performance and reproducibility of a laser fluorescence system for detection of occlusal caries in vitro,” Caries research, vol. 33, pp. 261-266.

[15] Gen Mayanagi 1, Koei Igarashi, Jumpei Washio, Nobuhiro Takahashi (2017), “pH response and tooth surface solubility at the tooth/bacteria interface,” Caries research, vol. 51.2, pp. 160-166.

[16] Ajani, S. N. ., Khobragade, P. ., Dhone, M. ., Ganguly, B. ., Shelke, N. ., & Parati, N. . (2023). Advancements in Computing: Emerging Trends in Computational Science with Next-Generation Computing. International Journal of Intelligent Systems and Applications in Engineering, 12(7s), 546–559

[17] I Kleinberg, G N Jenkins, R Chatterjee, L Wijeyeweera (1982), “The antimony pH electrode and its role in the assessment and interpretation of dental plaque pH,” Journal of Dental Research, vol. 61, pp. 1139-1147.

[18] Noriko Hiraishi, Yuichi Kitasako, Toru Nikaido, Satoshi Nomura, Michael F Burrow, Junji Tagami (2003), “Effect of artificial saliva contamination on pH value change and dentin bond strength”, Dental Materials, vol. 19, pp. 429-434.

[19] Keiko Murakami, Yuichi Kitasako, Michael F Burrow, Junji Tagami (2006), “In vitro pH analysis of active and arrested dentinal caries in extracted human teeth using a micro pH sensor,” Dental materials journal, vol. 25, pp. 423-429.

[20] Yuichi Kitasako, Nathan J Cochrane, Matin Khairul, Kanako Shida, Geoffrey G Adams, Michael F Burrow, Eric C Reynolds, Junji Tagami (2010), “The clinical application of surface pH measurements to longitudinally assess white spot enamel lesions,” Journal of dentistry, vol. 38, pp. 584-590.

[21] Mie Fujii 1, Yuichi Kitasako, Alireza Sadr, Junji Tagami (2011), “Roughness and pH changes of enamel surface induced by soft drinks in vitro-applications of stylus profilometry, focus variation 3D scanning microscopy and micro pH sensor,” Dental materials journal, vol. 30, pp. 404-410.

[22] Patle, Kamlesh S., Hemen K. Kalita, and Vinay S. Palaparthy (2022), “Reduced Graphene Oxide Soil Moisture Sensor with Improved Stability and Testing on Vadose Zone Soils,” Artificial Intelligence Driven Circuits and Systems. Springer, Singapore, pp. 115-123.

[23] Chindanai Ratanaporncharoen, Miyuki Tabata, Yuichi Kitasako, Masaomi Ikeda, Tatsuro Goda, Akira Matsumoto, Junji Tagami, Yuji Miyahara (2018), “pH mapping on tooth surfaces for quantitative caries diagnosis using micro Ir/IrOx pH sensor,” Analytical chemistry, vol. 90 pp. 4925-4931.